SMC-TR-05-08

Aerothermal Heating for Satellite Reentry Conditions

22 September 2004

Prepared by

R. G. STERN
Imagery Programs Division
National Systems Group

Prepared for

SPACE AND MISSILE SYSTEMS CENTER
AIR FORCE SPACE COMMAND
2430 E. El Segundo Boulevard
Los Angeles Air Force Base, CA 90245

Systems Planning and Engineering Group

20050112 052

**THE AEROSPACE
CORPORATION**
El Segundo, California

John R. Edwards
SMC/AXF

REPORT DOCUMENTATION PAGE

1. REPORT DATE (DD-MM-YYYY)	2. REPORT TYPE	3. DATES COVERED (From - To)
....22-09-2004		

4. TITLE AND SUBTITLE	5a. CONTRACT NUMBER
Aerothermal Heating for Satellite Reentry Conditions	FA8802-05-C-0001
	5b. GRANT NUMBER
	5c. PROGRAM ELEMENT NUMBER

6. AUTHOR(S)	5d. PROJECT NUMBER
Richard G. Stern	
	5e. TASK NUMBER
	5f. WORK UNIT NUMBER

7. PERFORMING ORGANIZATION NAME(S) AND ADDRESS(ES)	8. PERFORMING ORGANIZATION REPORT NUMBER
The Aerospace Corporation National Systems Group El Segundo, CA 90245-4691	TR-2004(8506)-2

9. SPONSORING / MONITORING AGENCY NAME(S) AND ADDRESS(ES)	10. SPONSOR/MONITOR'S ACRONYM(S)
Space and Missile Systems Center Air Force Space Command	SMC
2450 E. El Segundo Blvd. Los Angeles Air Force Base, CA 90245	11. SPONSOR/MONITOR'S REPORT NUMBER(S) SMC-TR-05-08

12. DISTRIBUTION/AVAILABILITY STATEMENT

Approved for public release; distribution unlimited.

13. SUPPLEMENTARY NOTES

14. ABSTRACT

Equations are presented which provide heating rates for objects reentering the Earth's atmosphere. The relationships are appropriate for estimating the survival or aerothermal breakup of a reentering vehicle. The relationships presented in this report predict heating which is an order of magnitude less than predicted by existing theory. The results presented in this report are based on numerous satellite reentry experiments conducted over the last three decades.

15. SUBJECT TERMS

16. SECURITY CLASSIFICATION OF:			17. LIMITATION OF ABSTRACT	18. NUMBER OF PAGES	19a. NAME OF RESPONSIBLE PERSON Richard G. Stern
a. REPORT UNCLASSIFIED	b. ABSTRACT UNCLASSIFIED	c. THIS PAGE UNCLASSIFIED		20	19b. TELEPHONE NUMBER (include area code) (310)336-4278

Contents

Figures

Tables

1 Introduction

Equations are presented which provide heating rates for objects reentering the Earth's atmosphere. The relationships are appropriate for estimating the survival or aerothermal breakup of a reentering vehicle. The relationships presented in this report predict heating which is an order of magnitude less than predicted by traditional theory.

The results presented in this report are based on numerous satellite reentry experiments conducted over the last three decades. Key insight into the aerothermal environment was afforded by the VAST (Vehicle Atmospheric Survivability Test) and VASP (Vehicle Atmospheric Survivability Project) experiments.

The repeatability of the observed breakup, hence aerothermal environment, was validated by several controlled reentries conducted during 1996 and 1997. The reentries involved monocoque and truss structures as well as satellite vehicles and launch vehicles (Agena stage attached to a payload) with their respective components.

The purpose of this report is to provide wider exposure of the results, which has been limited to a few Air Force programs.

2 History

Six satellite reentry tests were conducted over three decades ago (1971 – 1973). These tests were authorized by the Office of the Secretary of the Air Force (OSAF) at the request of White House staff members. The objective of the tests was limited to experimentally determining the reentry survivability and condition of vehicle payload elements. A by-product of the tests was an insight into a satellite's aerothermal breakup process.

The breakup phenomenon observed revealed that contrary to theory, breakup was essentially independent of attitude behavior and geometry. In addition, the heating encountered by the reentering satellite was an order of magnitude less than theory would indicate. These revelations were utilized in deboost and strategy policy for those Air Force Low Earth Orbiting (LEO) satellite vehicles directly under the OSAF.

For several decades, knowledge of the reentry tests remained limited to personnel involved with the OSAF's LEO programs. Academia, most satellite and launch vehicle contractors, and other government agencies remained unaware of the experiments.

In 1983 (a decade after the last reentry test), an OSAF Air Force satellite program was scheduled to be launched from Vandenberg AFB by the Space Shuttle. The satellite's mission profile and design required that it be launched into an elliptical orbit with almost a four hundred nautical mile apogee altitude. NASA analysis indicated that the mission could not be safely conducted since the STS's External Tank (ET) would reenter over the Pacific and the predicted breakup would be at a high enough altitude that its debris dispersion pattern would be excessive. At the direction of the OSAF, the STS program manager at JSC along with several key managers and selected astronauts were briefed on the VAST reentry experiment results. NASA management agreed to the Air Force

mission profile and would, subsequently, conduct tests to eventually verify the ET reentry breakup characteristics.

By 1991, a new type of satellite under the direction of OSAF was in operation and the program director wanted to readdress the requirement to deboost the satellite at the end of mission. He directed that a reentry experiment be planned to demonstrate the reentry survivability characteristics of the satellite. The experiment eventually took place in March 1997.

In an effort to theoretically address the survivability of the new satellite, the breakup of the satellites observed in the VAST's of 1971 were readdressed. The breakup sequence was determined and attendant heating relationships were developed. The type of satellites used in the experiments of the early 1970's were last operational in the mid 1980's.

Three additional satellite reentry experiments were conducted 25 years after the initial VAST experiment of 1971. The satellites were different than the vehicles used in VAST or VASP and performed different missions. Two of the satellites were deboosted from an orbit which yielded reentry velocities approaching Earth escape velocity. The two vehicles were primarily made up of a monocoque structure similar to the VAST vehicles. The third vehicle had reentry conditions similar to those of VAST and VASP but was different structurally. This third vehicle was primarily composed of truss structures (bridge like), whereas the vehicles of VAST and VASP were primarily monocoque (tube shaped). The results were consistent with the VAST results and extended the applicability of these results to entry from near parabolic entry conditions (velocity ≈ 34000 ft/sec) and down to velocities of several thousand ft/sec. A reentry experiment was also conducted with NASA's Compton Gamma Ray Observatory (CGRO) in the year 2000.

This document summarizes and updates the heating relationships and limitations developed from the experiments of the previous three decades.

3   VAST and VASP Experiments

The satellite reentry experiments conducted during the early 1970's involved two different types of satellite vehicles. The first four tests referred to as VAST (Vehicle Atmospheric Survivability Tests) utilized one specific type of satellite vehicle. A second and larger type of satellite vehicle was subsequently used in two tests referred to as VASP (Vehicle Atmospheric Survivability Project). Except for the last two VAST reentries, extensive tracking assets were employed and are summarized in Table 1.

Table 1 summarizes the Principal Assets used in VAST and VASP. One of two identical tracking ships ARIS (Advanced Range Instrumentation Ships) was in service while the second was being serviced. The ship could collect telemetry, radar and optical data. The optical data required clear skies. Optical data was fortuitously available in VAST2 and VASP 1. The IFLOT (Intermediate Focal Length Optical Tracker) could and did obtain image resolution of 1 ft near the point of closest approach.

The TRAP (Thermal Radiation Airborne Program) carried infrared equipment and visual range optics which tracked reentry and satellite breakup. A PRESS aircraft, similar to

5

TRAP, was operated by the Navy. A large land based radar at Shemya, Alaska was used when the reentry trajectory path allowed (VAST 1 and VASP 1).

The support summary for the tests is shown in Table 2. Limited support was provided for VAST 3 and 4 since these were payload element retrieval missions. Therefore, on VAST 3 and 4 no tracking of the breakup process was made. The breakup histories of VAST were so consistent that only two VASP tests were planned for the larger vehicle (which was significantly different structurally). The first VASP test confirmed the breakup characteristics, which were predicted from VAST results. VAST 1 and VAST 2 were targeted for reentry in the Western Pacific because of range safety and observation considerations. It is noted that the debris footprint for VAST ranged up to one thousand nautical miles. It was the intent of VAST 1, 2 and 4 to stay off populated land masses. VAST 3 was a payload sensor recovery mission targeted into a remote region of Alaska. VAST 4 was intended to be a payload element recovery mission and that portion of the 1000 nmi long footprint was targeted for Eniwetok Lagoon. VASP 1 was targeted into the Western Pacific to utilize the large radar at Shemya, Alaska. The second and final VASP was targeted for payload element recovery in Eniwetok Lagoon. The support for the second VASP had significant tracking to confirm that breakup was consistent with VASP 1, as well as the VAST reentries.

The PRESS Aircraft used in VAST 2 was a Navy version of the TRAP aircraft. As can be noted in Table 2, both VAST 1 and 2 had the support of two optical tracking aircraft. By 1973 only one optical tracking aircraft was available for the two VASP reentries. The data obtained from that single TRAP on VASP 2, however, was remarkable and extremely informative.

3.1 The Vehicle Atmospheric Survivability Tests (VAST)

The Vehicle Atmosphere Survivability Tests (VAST) were performed upon reentering satellite vehicles subsequent to a controlled deboost. The tests were unique as the satellite utilized was a dual vehicle with a weak mechanical linkage which allowed separation into two components of nearly equal size and surface material. Two objects with different attitude histories were observed reentering through the same atmosphere allowing attitude effects to be evaluated. The entry conditions were representative of those attendant with a reentry resulting from orbit decay. The results indicated that: (1) objects reentering the Earth's atmosphere are far more survivable than predicted by traditional analytic theory and (2) that thin-walled materials consistently resisted melting in environments nearly an order of magnitude more severe than predicted. Theory would indicate that attitude and size are significant factors in the heating that an object experiences. The experimental data indicate that these effects are also less than theorized. Empirical convective heating relationships were developed based upon the VAST breakup sequences. The relationships have been applied to many subsequent reentries involving both controlled deorbits and those resulting from orbital decay and found to be in agreement with observations.

3.1.1 Vehicle Description

The vehicle used in the VAST tests was an Agena D attached to a payload section of the same size. The Agena D was used as the final stage of a Titan III B / Agena D launch vehicle. After the Agena D made the orbit insertion burn, it remained attached for the

6

orbital and reentry phases of the mission. The Agena provided control, communication, command, orbit adjust, attitude control and power for the attached payload section.

The payload structural attachment to the payload was substantial during the launch phase of the mission when loads are great. After orbit insertion, the attachment was removed leaving the payload attached to the Agena by a very weak mechanical tie.

The Agena D generally consists of three sections (see Figure 1): the Forward Rack, the Tank and Propulsion Section, and the Aft Rack. A special equipment section (SEC) was rigidly attached to the Agena Forward Rack which contained most of the batteries, payload peculiar mechanisms, command and power outlets to the payload section and a very weak mechanical attachment to the payload section. The attachment was designed to resist only relatively small aerodynamic and attitude control loads. It could accommodate axial propulsive orbit adjust and deboost loads.

The payload had an aluminum monocoque structure 23.7 ft long and 5 ft in diameter. The payload's external monocoque structure was anodized aluminum 0.10 in thick. The Agena vehicle with the SEC was 22.2 ft long. The Agena had a cylindrical monocoque aluminum Forward Rack and Special Equipment Compartment (SEC) attached to an anodized aluminum propellant tank section 0.12 in thick and connected in turn to an Aft Rack with a truss structure surrounding the Agena's main engine.

3.1.2 Vehicle Breakup Sequence

The detailed breakup sequence of the vehicles used in VAST was derived from offboard sensor information. The physical make-up of the vehicles tested was fortuitous since thin-walled structures utilizing aluminum were employed. Aluminum truss structures were also utilized. The significance of the thin-walled structure is that in conjunction with the shallow flight path angles (relative flight path angles less than 0.5 deg), the temperatures achieved were dictated by radiation equilibrium considerations. When the radiation equilibrium temperature (heat input equal to heat radiated from the body) reached the material's melting temperature, the structure lost all structural integrity and hence "broke up" under very low aerodynamic loading. The breakup sequence identified is summarized in the following paragraphs and Table 3.

The vehicles employed in VAST 1 and VAST 2 were deboosted from Low Earth Orbit with the Agena's engine pointing towards the incident airstream (aligned with the local horizontonal). The cold gas attitude control system maintained this orientation as long as possible. VAST 1 remained stable (engine forward) until the Agena's Aft Rack broke up and separated from the main body. The failure of the rails (Truss Structure, see Figure 1) caused the attitude control elements (thrusters, nitrogen gas tanks) to separate thereby terminating attitude control. On VAST 2 attitude control, gas was expended prior to reentry and the vehicle tumbled. The failure of the Aft Rack on VAST 1 occurred with the airflow parallel to the rails whereas with the tumbling VAST 2, the rails for the most part were normal to the airflow.

Subsequent to the loss of the Aft Rack, the payload and attached Agena tumbled on both VAST 1 and VAST 2. The weak mechanical tie mentioned earlier in Section 3.1.1 could not maintain structural integrity between the Agena and payload and they separated.

7

Based on ARIS radar data, the Agena section with its massive Special Equipment Compartment (SEC) quickly stabilized with that section facing into the incident airstream on both VAST 1 and VAST 2. As observed by radar, the Agena tank wall on both VAST 1 and VAST 2 subsequently melted separating the Forward Rack and attached SEC from the main engine, which continued on separately.

Once separated from the Agena the payloads on VAST 1 and VAST 2 stabilized and oscillated at a near broadside attitude. Attitudes were deduced by radar and optical information obtained from ARIS. The incident airflow was nearly normal to the payload's outer structure. In both instances the payload's outer monocoque structure failed as the melting temperature was achieved releasing the internal subcomponents. Excellent optical coverage of VAST 2 (from ARIS) indicated that the outer structure experienced a massive and sudden thermal melting failure on both windward and leeward (opposite incident airstream) faces.

3.1.3 Vehicle Melting and Attendant Heating Rates

The melting of the outer payload structure and Agena tank sections are a very good indicator of the heating rate experienced by the vehicle, since radiation equilibrium dictates this temperature and structural loads are low. The load factor at vehicle breakup is less than unity. Also, the loss of structural strength due to elevated temperature is time dependent, so the structure should maintain its integrity as the melt point is approached. Tables 3 and 5 provide attitude, dynamic pressure, altitude and stagnation point heating rates at various events. For radiation equilibrium, the heating rate to melt anodized aluminum with an emissivity of 0.8 (Reference 1) is 3.032 BTU/ft^2/sec [see Eq. (7) to follow]. Table 3 provides heating rates utilizing a traditional relationship. From Table 3 the surfaces either normal or parallel to the flow did experience an order of magnitude less heating than would be calculated from the reference stagnation heating rate. The traditional stagnation heating rate $\dot{Q}_{STAG}$ obtained from Reference 2 is as follows.

$$\dot{Q}_{STAG} = \frac{1.068}{\sqrt{R}}\left(\frac{\rho}{\rho_{SL}}\right)^{0.5}\left[\frac{V}{1000}\right]^3$$

$\dot{Q}_{STAG}$ = Stagnation Heating Rate ($BTU/ft^2/sec$)

$\dfrac{\rho}{\rho_{SL}}$ = Ratio of atmospheric density at altitude to that at sea level

V = Velocity (ft/sec)

R = Nose Radius (ft)

(1)

The reference stagnation heating rates of Table 3 are based on a one-foot reference radius sphere whereas the radius of the payload section and tank are both 2.5 ft. Based on Eq. (1), this theoretically should further reduce the heating by 37% $\left(\sqrt{\dfrac{1}{2.5}} = .63\right)$. The heating rates of Table 3 are still an order of magnitude greater than what is required to melt the aluminum payload. The payload was normal to the flow and should represent

stagnation heating. The ratio for heating rates parallel to the flow (when the Agena tank melts) compared to normal to the flow (when the payload section melts) is as follows for each of the two tests.

$$\text{Ratio} = \frac{\text{Payload Outer Structure (Airflow Normal to Surface)}}{\text{Agena Tank Section (Airflow Parallel to Surface)}}$$

$$\text{VAST 1 Ratio} = \frac{98.6 \ BTU/ft^2/sec}{107.3 \ BTU/ft^2/sec} = 0.92 \qquad \text{VAST 2 Ratio} = \frac{95.2 \ BTU/ft^2/sec}{107.1 \ BTU/ft^2/sec} = 0.89 \qquad (2)$$

This yields only an eight to eleven percent reduction for flow, which is parallel to the surface, far short of the traditional factor of seven or greater for side heating.

The Agena Aft Rack truss structure was built up of thin aluminum rails and tubing several inches across. The effective heating that an object experiences is theoretically inversely proportional to the square root of a reference radius Eq. (1). This suggests that rails would achieve melting temperature at about one-fifth the reference stagnation heating that melted the tank and payload outer structure. The flow on VAST 1 was parallel to the rails at failure, whereas on VAST 2 it was normal. The ratio of the normal-to-parallel stagnation heating required to achieve melting/failure of the rack rails is

$$\text{Ratio} \quad \frac{\text{VAST 2 Normal Flow}}{\text{VAST 1 Parallel Flow}} = \frac{69.8 \ BTU/ft^2/sec}{75.5 \ BTU/ft^2/sec} = 0.92 \qquad (3)$$

The above ratio is consistent with the normal to parallel heating relationships where the airflow on the payload outer structure is normal and the airflow on the Agena tank is parallel. The ratio of 0.92 is incredibly close to the ratios of Eq. (2) indicating that contrary to theory little heating relief occurs for side heating.

Next, the effect of heating on a structure with relatively small radius will be addressed. The rails on the Agena's Aft Rack represent such structure. On VAST 2 the rails were normal to the flow at failure and occurred at a reference heating rate of 69.8 BTU/ft^2/ sec compared to the normal flow on the payload of 95.2 BTU/ft^2/sec. The factor for increased heating on the rails may be deduced to be:

$$\text{Ratio} = \frac{95.2 \ BTU/ft^2/sec}{69.8 \ BTU/ft^2/sec} = 1.36 = \frac{1}{0.73} \ \text{[Flow Normal to Structure]} \qquad (4)$$

On VAST 1 the flow was parallel to the rails at failure. The reference heating rates at failure for the rails was 75.5 BTU/ft^2/ sec and the failure of the Agena tank (parallel flow) was 107.3 BTU/ft^2/ sec.

$$\text{Ratio} = \frac{107.3 \ BTU/ft^2/sec}{75.5 \ BTU/ft^2/sec} = 1.42 = \frac{1}{0.70} \ \text{[Flow Parallel to Structure]} \qquad (5)$$

The rails are several inches in diameter while the Agena Tank or payload section to which comparisons are made have a 5.0 ft diameter. Again, the theoretical effect of radius (Eq. 1) varies as the inverse of the square root of radius. The rails have 1/30 (i.e. 1 in/30 in) the radius of the tank or payload section therefore the heating required to melt the rails should be a factor of 5.5 less than for the Agena tank or payload section

9

rather than the factor of 1.4 observed in the above ratios (Eqs. 4 and 5). The VAST experiments demonstrate that aerodynamic heating is only weakly affected by geometry or attitude. The effect, although small, was consistent.

It is evident that the heating at a failed surface is much different than estimated by traditional methods. Furthermore, the effect of geometry also appears to be much less influential than traditional methods would predict. The analytic results of References 3 thru 6, which address the entry of meteors into planetary atmospheres, surprisingly show results not unlike those observed in VAST I and VAST II. The similarity rests in that the stagnation point heating normal to flow is almost an order of magnitude less than traditional convective heating analysis would predict. Also, the heating on the objects' side is hardly different than at the stagnation point. While the entry conditions and atmospheric physics associated with the planetary entry of meteors is much different than that of a reentering satellite, the analysis of meteor reentries are of interest and might provide an insight to the gross over-prediction of heating that reentering satellites experience.

It is fortuitous that in both VAST experiments two objects are reentering simultaneously at different attitudes. The Agena is trimmed out front end into the velocity vector [with the engine trailing (see Figure 1)] while the payload is nearly broadside. The heating rate, which produces melting on a surface parallel to the flow, is 0.89 [Eq. (2)] of the surface normal to the flow. Noting as before that the radius is a very weak if nonexistent factor for satellite reentries, we will neglect the radius effect in the development of a stagnation heating equation. Neglecting the effect of radius, the reference stagnation heating rate provided in Table 3 is 98.6 and 95.2 BTU/ft^2/sec when the broadside payload melted.

Using the heating rate relationship of Eq. (1) with a one-foot reference radius, we have the heating rate for the VAST 2 payload section.

$$\dot{Q}_{STAG} = 1.068 \left(\frac{\rho}{\rho_{SL}}\right)^{0.5} \left(\frac{V_R}{1000}\right)^3 = 95.2 \; BTU/ft^2/sec \; (VAST \; 2) \tag{6}$$

The shallow entry angle placed the vehicle at or near radiation equilibrium conditions, which dictated that the anodized aluminum experienced a heating rate of 3.032 BTU/ft^2/sec in order to achieve melting temperature (1680°R). That heating rate is determined as follows

$$\dot{Q} = \varepsilon\sigma T^4$$
$\dot{Q}$ = Radiation Heat Loss (BTU / ft^2/ sec)
T = Aluminum Melting Temperature (1680 degrees Rankine) (7)
ε = Emissivity (0.8 anodized aluminum)
σ = Stephen Boltzman Constant $\left(4.7583 \times 10^{-13} \; BTU / ft^2/ sec\right)$

Then,

$\dot{Q}$ = 3.032 BTU/ft^2/ sec

Therefore, the proper stagnation heating indicator should be a factor 31.39 $\left(\dfrac{95.2}{3.032}\right)$ less than Eq. (6). By reducing the constant of 1.068 in Eq. (6) by 31.39, we have:

$$\dot{Q}_{STAG} = 34.02\left(\frac{\rho}{\rho_{SL}}\right)^{0.5}\left(\frac{V}{10000}\right)^3 \tag{8}$$

Radius is not included in Eq. (8) since radii are large (R > 1 ft) and as discussed previously not a significant factor. The heat input for the sides of the Agena at the time the aluminum walls melt is 0.92 as conservatively (higher value) deduced from Eq. (2). For side surfaces, the heating calculated from Eq. (8) should be reduced by 0.92. Also, noting that the effect for the small radius of the Aft Rack rails was only about 40 percent higher than stagnation, it can be used to estimate the effect on small radius objects. The preceding results are summarized in Table 4. Using the relationships of Table 4, the appropriate heating rates at significant VAST events are presented in Table 5. As is seen, excellent consistency in melting conditions is achieved.

3.2 The Vehicle Atmospheric Survivability Project (VASP)

The satellite vehicle used in the VASP tests was larger and of relatively simple monocoque structure (not a dual vehicle as was VAST). The vehicle did have a boatail, which resulted in a trim angle of attack of 19° (verified by onboard telemetry). Until initial breakup (loss of boatail), the vehicle was generating lift. While the lift corrupted the trajectory, the vehicle reached the melting temperature at conditions in accordance with the VAST breakups. Further corroboration of the VAST results was obtained through onboard temperature data obtained prior to breakup, which indicated heating an order of magnitude less than obtained by traditional heating analysis.

The VASP 1 breakup was consistent with VAST breakup conditions. The reentry breakup allowed the estimation of the trajectories of the payload elements for which recovery was desired. VASP 2 was targeted such that the desired components would nominally impact in or near Eniwetok Lagoon. The tracking resources of VASP 2 verified that its breakup was similar to VASP 1 and all of the VAST reentries. For this reason the VASP results were only used to confirm similarity to the VAST results.

4   Other Reentry Experiments

Two satellites were deboosted from highly elliptical orbits in the year 1996. These deorbits were monitored by the COBRA JUDY radar tracking ship (similar to ARIS) on one reentry and a COBRA BALL optical tracking aircraft (similar to TRAP) on both reentries. The vehicle's observed aerothermal breakup was as predicted by Eq. (8). The reentry velocity was 33 percent higher than for the VAST and VASP reentries. This is significant since Eq. (8)'s applicability is demonstrated over a range of velocities up to escape velocity.

Another satellite was deorbited and observed by a COBRA BALL aircraft in the year 1997. Unique in this test was the survival of a solar panel, which was tracked down to a terminal velocity of several thousand ft/sec where it then exited the tracker's field of view.

NASA's Compton Gamma Ray Observatory (CGRO) was deorbited in the year 2000 and observed by a COBRA BALL aircraft. Metric tracking of objects was not as prolific as in previous TRAP and COBRA BALL observations due to some camera modifications made prior to the flight. Based on analysis of a hand held video (used only on the CGRO reentry), the breakup did appear to be consistent with what Eq. (8) predicted for aerothermal breakup.

5   General Observations

The predicted heating using the equations of Table 4 is very similar to the heating predicted in References 3 through 6, which considered a strong shock wave associated with planetary entry of comets. The similarity with the VAST results is that stagnation heating is about an order of magnitude less than predicted with traditional methods. Also, the heating on the side of the object is only reduced from stagnation heating by about 10 percent. The bow shock as observed via infrared or radar is greater than 50 times that of the hard body. This generally unanticipated large bow shock may be associated with the reduced heating, which the hard body is receiving. The similarity with the heating predictions of References 3 thru 6 may be associated with the very large bow shock. The concern here is that the optically observed wake generally dims out at altitudes between 25 and 30 nmi even though the object still persists on radar. This baits the question: has heating as predicted by the relationships of Table 4 been terminated? The dimouts are well after peak heating but if reduced heating (Table 4) was also to cease, an order of magnitude increase in heating could be possible. Such an increase could then cause temperatures in excess of the melting temperature of materials like magnesium or aluminum.

The largely aluminum solar array reentry in the year 1997 survived down to a velocity of several thousand ft/sec where the aerothermal heating was very low. The observed object's wake was large, indicating the existence of a large bow shock down to an altitude under 136,000 ft (where it passed out of the sensor field of view).

Numerous objects have been recovered which would not be expected to survive unless heating attendant with the VAST equations (Table 4) existed throughout reentry. The equations of Table 4 may apply throughout reentry for some objects. As an example, circuit boards with color codes on resistors have been retrieved.

A large electric motor was observed on radar during VASP 1. The motor melted and dispersed a field of copper dipoles resulting from metal copper droplets. The bow shock diminished at about 30 nmi altitude and ended the applicability of Table 4. It is noted that had the motor continued to receive heating in accordance with Table 4 it would not have achieved melting temperatures.

The Agena engine on VAST 2 as it broke free and tumbled was visible to tracking cameras (the wake). As it stabilized, the optical track disappeared while radar coverage continued until it exited the radar's narrow beam. If the relative size of the bow shock is an indicator of reduced heating then one could assume that as the engine stabilized (exit cone trailing) the bow shock disappeared and it became subject to increased heating which could melt the engine. Continued radar track of the engine was not achieved and it cannot be established that melting eventually occurred. It is noted that of the

numerous Agena's which have inadvertently reentered, no engines have been found while numerous titanium pressurization vessels have been recovered.

A massive payload element from the VAST tests had a high ballistic coefficient (weight to drag ratio of 55 lb/ft^2) and was aerodynamically unstable. The higher the ballistic coefficient (weight to drag ratio), the higher the peak heating rate (see Figure 2). The payload element was observed to tumble by radar and fighter aircraft chase planes. The object was retrieved after impact and was undamaged by aerodynamic heating. This large unstable object with a high ballistic coefficient should have melted using traditional heating equations whereas Table 4 would predict survivability.

Table 4 equations are independent of a satellites vehicle's size. The reduced heating probably is attendant with a relatively large bow shock, which generally appears to be present down to an altitude of around 30 nmi. With higher ballistic coefficients, the heating rate will increase as altitude decreases. This coupled with the loss of the reduced heating associated with Table 4 would cause items with high ballistic coefficients (low drag) to melt. If very low ballistic coefficient objects experienced VAST heating rates (Table 4) down to 30 nmi they would survive with or without continued reduced heating.

6 Conclusions

Traditional relationships do not accurately predict satellite aerothermal heating. The simple relationships of Table 4 accurately predict satellite aerothermal heating and hence breakup. The relationships of Table 4 have been substantiated by reentries over the past three decades and should be used to determine debris impact locations and dispersions.

The equations have been substantiated with entry velocity from low Earth orbits to those approaching Earth escape velocity. Escape velocities are representative of a satellite deboost from a Molniya orbit. Escape velocity may also be achieved with a natural decayed reentry from a Molniya orbit, in which periodic orbit adjusts had not been maintained (i.e., dead satellite) and Sun/Moon perturbations cause a rapid loss of perigee altitude. The equations of Table 4 are applicable for deboost or decay from any Earth orbit since reentry at escape velocity represents the maximum achievable. Higher velocities would have to arise from an interplanetary or lunar return. The equations might not be applicable at interplanetary reentry velocities.

The regions within the Earth's atmosphere, to which the equations apply, are related below:

Altitude Range	Table 4 Applicability
30 nmi and above	Always
Below 30 nmi	(1) Large bow shock expected
	(2) For conservative estimates of surviving debris

The determination of the survivability of debris from a reentering satellite should use the equations of Table 4 down to impact. The results could be conservative in that objects which lose the large bow shock and the reduced heating predicted in Table 4 may not survive even though its predictions would indicate otherwise.

13

The equations of Table 4 can be used in the thermal design analysis of vehicles which are to reenter the atmosphere from Earth orbit. The applicability of Table 4 in design work should conservatively be limited to altitudes above 30 nmi where the applicability of the equations of Table 4 are persistent.

References

1. *Satellite Thermal Control Handbook*, Spacecraft Thermal Department, The Aerospace Corporation, 1994.

2. *The Generalized Trajectory Simulation System*, Volumes 1-5, Aerospace Report No. TR-0075(5549)-1, June 1975.

3. Lyne, J. E., Tauber, M. E., and Fought, R. M., *An Analytical Model of the Atmospheric Entry of Large Meteors and Its Application to the Tunguska Event*, The Journal of Geophysical Research, Vol. 101, No. E10, pp. 23207-23212, 1996.

4. Lyne, J. E. and Tauber, M. E., *The Tunguska Event*, Nature, Vol. 375, No. 6533, pp.638-639, 1995.

5. Lyne, J. E., Tauber, M. E., and Fought, R. M., *A Computer Model of the Atmospheric Trajectory of the Tunguska Object*, invited presentation at the International Tunguska '96 Workshop, Bologna, Italy, July 15-17, 1996.

6. Lyne, J. E. and Tauber, M. E., *An Analysis of the Tunguska Event*, AIAA Paper 95-3477, presented at the 1995 AIAA Atmospheric Flight Mechanics Meeting, Baltimore, MD, August 1995.

7. Stern, R. G., *Analysis of Mir Reentry Breakup*, Aerospace Report No. TR-2003(8506)-1 dated 11 February 2003.

Table 1. Principal Resources

ARIS TRACKING SHIP

    Radar ~ L Band ~ C Band ~ UHF

    Optics ~ Boresight Cameras ~IFLOT

    Telemetry – 30 ft. Dish (225 → 2300 mhz)

TRAP AIRCRAFT – OPTICAL TRACKING

    TRAP 1

    TRAP 7

ARIA TELEMETRY AIRCRAFT

LAND BASED RADARS

    Shemya, Alaska

    Clear

MISCELLANEOUS SUPPORT

    Sonobuoys

    Cubmarine Underwater Recovery

    USN Watertown Surface Recovery

Table 2. Support Summary

VAST / VASP	Vehicle	Date	Payload Impact	ARIS	TRAP	ARIA	Land Based Radar	Other
VAST 1	OM 30	9 Feb 71	BOA*	1	2	2	Shemya	USN Watertown
VAST 2	OM 31	13 May 71	BOA*	1	1	2	--	PRESS Aircraft
VAST 3	OM 32	3 Sept 71	Alaska	--	--	--	Clear	--
VAST 4	OM 34	11 April 72	Eniwetok	--	--	--	--	Sonobuoys
VASP 1	SV 5	19 May 73	BOA*	1	--	2	Shemya	--
VASP 2	SV 6	12 Oct 73	Eniwetok	1	1	3	--	Sonobuoys & Cubmarine

*Broad Ocean Area

Table 3. Comparison of VAST Conditions at Significant Events

Event (Material which Failed)	VAST 1				VAST 2			
	Altitude (nmi)	Attitude	Stagnation Heating Rate* (BTU/ft²/sec)	Dynamic Pressure (lb/ft²)	Altitude (nmi)	Attitude	Stagnation Heating Rate* (BTU/ft²/sec)	Dynamic Pressure (lb/ft²)
Aft Rack Truss Separation (Aluminum Tubing)	43.5	Stable α = 180°	75.5	12.2	43.76	Tumbling	69.8	10.9
Payload/Agena Separation	42.2	Tumbling	87.7	17.7	41.33	Tumbling	96.3	22.1
Agena Tank Melts (Thin Aluminum Wall)	40.49	Aluminum Wall Nearly Parallel to Flow	107.3	27.7	40.38	Aluminum Wall Nearly Parallel to Flow	107.1	28.3
Payload Outer Structure Melts (Aluminum Shell)	41.15	Oscillating (Nearly Broadside)	98.6	23.14	40.54	Oscillating (Nearly Broadside)	95.2	25.3

$$*\dot{Q}_{STAG} = 1.068 \left(\frac{\rho}{\rho_{SL}}\right)^{0.5} \left(\frac{V}{1000}\right)^3 \quad \text{(One-Foot Reference Radius)}$$

16

Table 4. VAST Empirical Heating Rates

- **Stagnation Point Heating** $\dot{Q}_{STAG}$

$$\dot{Q}_{STAG} = 34.02 \left(\frac{\rho}{\rho_{SL}}\right)^{0.5} \left(\frac{V}{10000}\right)^3 \text{ BTU/ft}^2 \text{/sec}$$

$\dfrac{\rho}{\rho_{SL}}$ = Ratio of Atmospheric Density at Altitude to that at Sea Level

V_R = Relative Velocity (ft/sec)

- **Side Heating** $\dot{Q}_{SIDE}$

$$\dot{Q}_{SIDE} = 0.92 \ \dot{Q}_{STAG}$$

- **Effect of Radius**
  - No Increase for Most Radii
  - For Radius < 2", <u>Increase</u> Heating by 40%

Table 5. Comparison of VAST Empirical Heating Rates at Significant Events

Event (Material which Failed)	VAST 1				VAST 2			
	Altitude (nmi)	Attitude	Stagnation Heating Rate* (BTU/ft²/sec)	Heating Rate at Failed Surface (BTU/ft²/sec)	Altitude (nmi)	Attitude	Stagnation Heating Rate* (BTU/ft²/sec)	Heating Rate at Failed Surface (BTU/ft²/sec)
Aft Rack Truss Separation (Aluminum Tubing)	43.5	Stable α = 180°	2.40	2.98	43.76	Tumbling	2.22	3.11
Agena Tank Melts (Thin Aluminum Wall)	40.49	Aluminum Wall Nearly Parallel to Flow	3.42	3.04	40.38	Aluminum Wall Nearly Parallel to Flow	3.41	3.03
Outer Barrel Melts (Aluminum Shell)	41.15	Oscillating Low Angle of Attack	3.14	2.78 to 3.14	40.54	Tumbling (Nearly Broadside Attitude)	3.03	3.03

$$*\dot{Q}_{STAG} = 34.02 \left(\frac{\rho}{\rho_{SL}} \right)^{0.5} \left(\frac{V}{10000} \right)^3 \quad \text{(Independent of Radius)}$$

Heating Rate Required to Achieve Radiation Equilibrium Melting Temperature of Anodized Aluminum = 3.03 BTU/ft²/sec
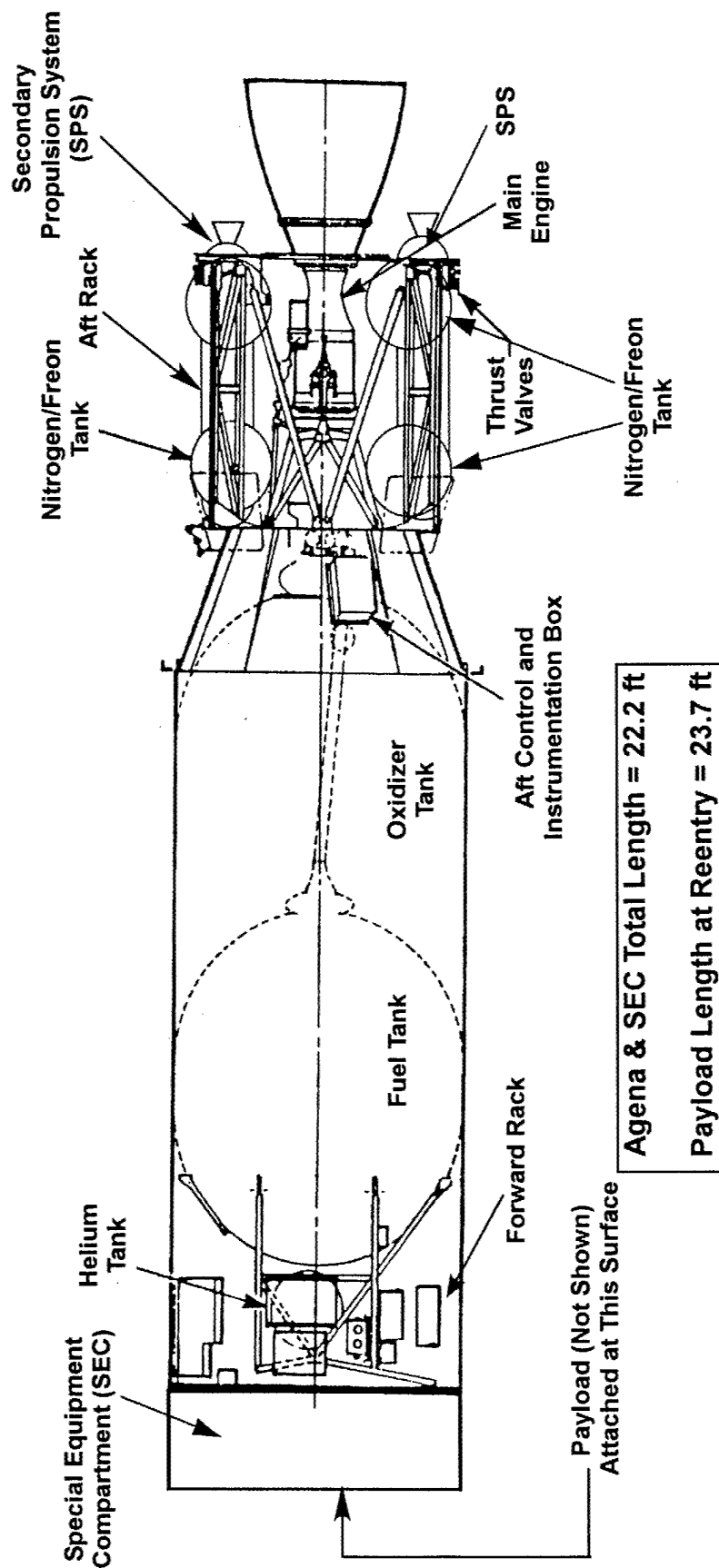
Figure 1. Agena Configuration Used in VAST

Secondary Propulsion System (SPS)

SPS

Main Engine

Aft Rack

Nitrogen/Freon Tank

Thrust Valves

Nitrogen/Freon Tank

Aft Control and Instrumentation Box

Oxidizer Tank

Fuel Tank

Forward Rack

Helium Tank

Special Equipment Compartment (SEC)

Payload (Not Shown) Attached at This Surface

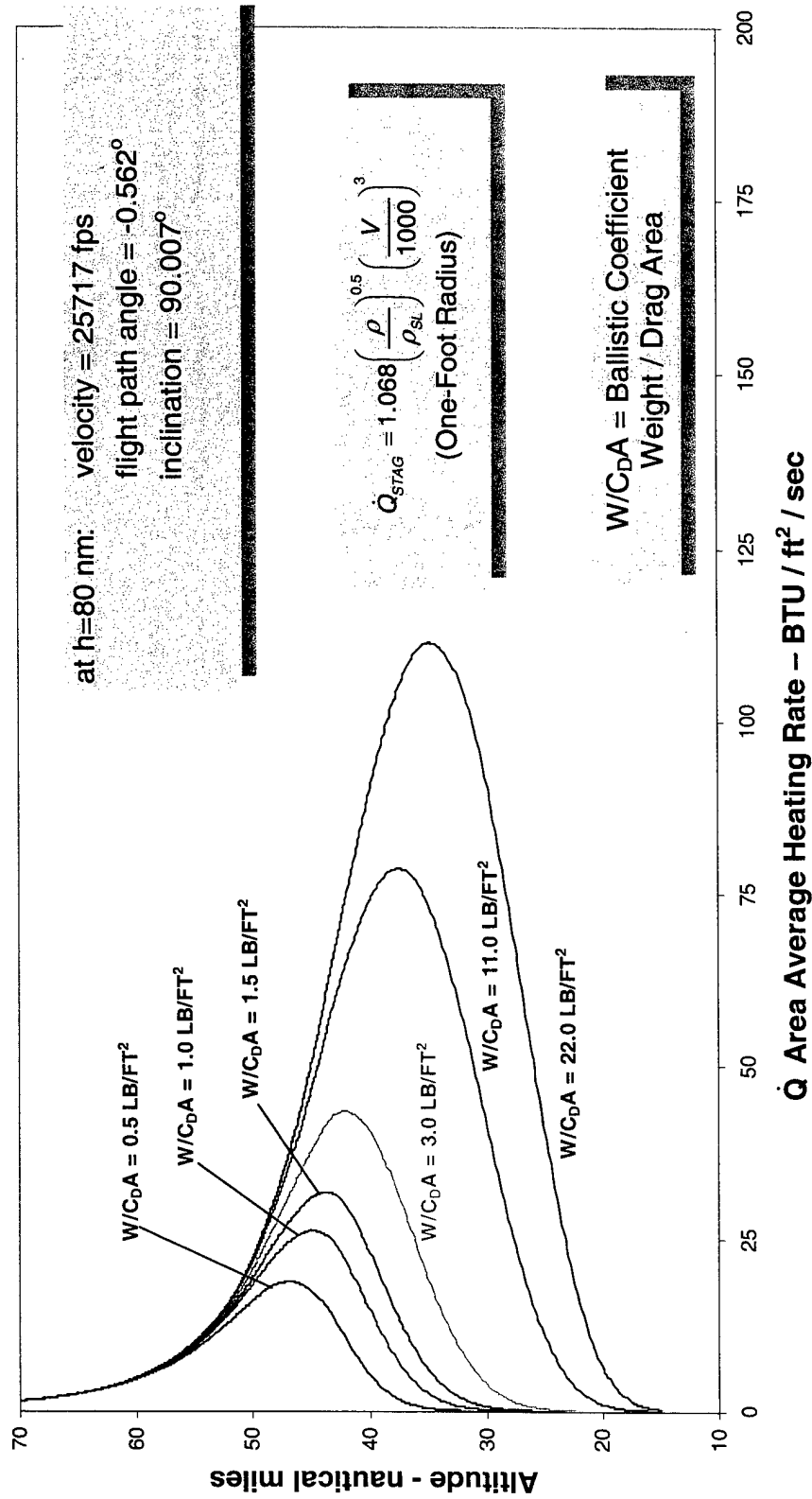Agena & SEC Total Length = 22.2 ft

Payload Length at Reentry = 23.7 ft

19

Figure 2. Effect of Ballistic Coefficient Upon Traditional Heating Rates

20